Inorganic Materials, Vol. 41, No. 8, 2005, pp. 840–844. Translated from Neorganicheskie Materialy, Vol. 41, No. 8, 2005, pp. 960–965.
Original Russian Text Copyright © 2005 by Skrobot, Ugolkov, Grebenshchikov, Gusarov.

Subsolidus Phase Relations in the System Dy_2O_3–Rh_2O_3

V. N. Skrobot, V. L. Ugolkov, R. G. Grebenshchikov, and V. V. Gusarov

Grebenshchikov Institute of Silicate Chemistry, Russian Academy of Sciences,
ul. Odoevskogo 24/2, St. Petersburg, 199155 Russia

e-mail: skrobot@mail.ru

Received December 20, 2004

Abstract—The Dy_2O_3–Rh_2O_3 system is studied by thermal analysis, x-ray diffraction, and chemical analysis of annealed and quenched samples. The results are used to construct a schematic subsolidus phase diagram of the system. Only one double oxide, $DyRhO_3$, is obtained. Some of its physicochemical properties are reported.

INTRODUCTION

This article presents the continuation of our studies concerned with phase relations in Ln_2O_3–Rh_2O_3 (Ln = rare-earth metal) systems [1–6], which are motivated by the interesting properties of compounds in these systems. First, compounds with the general formula $LnRhO_3$ are used in catalysis and electrochemistry. In particular, $LaRhO_3$ is a catalyst for the hydrogenation of carbon monoxide to methane, acetaldehyde, and ethanol [7]. In addition, electrolytic cells with $LuRhO_3$ ceramic cathodes achieve powers and photovoltages sufficient for water photoelectrolysis by solar radiation, with no applied potential [8]. Second, both $LnRhO_3$ and $LnM_{1-x}Rh_xO_3$ (M = 3d transition metal) phases have perovskite-like structures and offer a wide variety of electrical and magnetic properties. For example, $LaNi_{1/2}Rh_{1/2}O_3$ is a semiconductor exhibiting Pauli paramagnetism in the range 40–300 K and passes into a spin glass state below 10 K [9], whereas $LaMn_{1/2}Rh_{1/2}O_3$ combines semiconducting and ferromagnetic properties [10]. $LaMn_{0.976}Rh_{0.024}O_{3.15}$ effectively catalyzes three reactions in NO + CO + C_3H_6 mixtures: reduction of NO and oxidation of CO and C_3H_6 [11]. Third, some of the mixed oxides in Ln–M–Rh–O (M = alkaline-earth metal) systems possess unusual crystal-chemical, electrical, and magnetic properties (see, e.g., [12–14]), which suggest that such systems may contain superconductors.

The first report that the Dy–Rh–O system contains a mixed oxide of composition $DyRhO_3$ appeared in 1970 [15]. Later, the synthesis, crystal chemistry, and physicochemical properties of this compound have been the subject of many studies [15–21], but the phase relations in the Dy–Rh–O system have yet not been investigated.

The purpose of this work was to study the phase relations in the Dy_2O_3–Rh_2O_3 system in air at temperatures of up to 1600°C and to construct the subsolidus phase diagram of this system.

EXPERIMENTAL

The starting materials used were 99.9+%-pure Dy_2O_3 and pure-grade $RhCl_3 \cdot 4H_2O$. When exposed to atmospheric oxygen for a long time at temperatures from 650 to 700°C, the latter compound oxidizes to the metastable phase α-Rh_2O_3, which has the corundum (hexagonal) structure [22]. The stable high-temperature polymorph β-Rh_2O_3, which has an orthorhombic corundum-like structure [23], was prepared by two procedures. In one of them, α-Rh_2O_3 was heat-treated in air at 800–950°C. In the other procedure, fine-particle rhodium metal was oxidized at 950–1000°C in air or flowing oxygen for at least 20 h. Fine-particle rhodium (rhodium black) was prepared by reducing an $RhCl_3$ solution in HCl with metallic zinc.

In our phase-diagram studies, we used mixtures of Dy_2O_3 and α-Rh_2O_3 in the molar ratios 9 : 1, 4 : 1, 3 : 1, 2 : 1, 3 : 2, 1 : 1, 3 : 5, 1 : 2, 1 : 3, 1 : 4, and 1 : 9 and also an equimolar mixture of Dy_2O_3 and fine-particle rhodium. After grinding and homogenization in a jasper mortar with ethanol, the mixtures were dried in air and then fired in corundum crucibles between 600 and 1600°C in 100°C steps. Some of the mixtures, including the equimolar composition, were fired and quenched in 10 to 20°C steps. The firing duration was 150 h at 1000°C and 75 h at higher temperatures. Every 20 h, the samples were reground and homogenized. At 1000°C and lower temperatures, we used an SNOL-I4 electric furnace. At higher temperatures, the samples were fired in a Pt–30% Rh wound quenching electric furnace. The firing and quenching steps were performed in air. The temperature was monitored with standard Pt/Pt–10% Rh (TPP-0555) or Pt–6% Rh/Pt–30% Rh (TPR-0679-01) thermocouples. During firing, the temperature was maintained constant with an accuracy of ±5°C or better using a VRT-3 temperature controller.

The phase composition of the starting mixtures and samples after firing and quenching was determined on a DRON-3 (Ni-filtered CuK_α radiation) or Siemens D 500 HS (CuK_α radiation, graphite monochromator) diffractometer. Measurements were made in the range $2\theta = 10°–95°$ with a scan step of 0.02° and a counting time of 1 s per data point.

Thermal analysis (DTA + TG + DTG) was carried out in air with a MOM C system (Hungary) at temperatures of up to 1200°C and with a SETARAM V-70 system (France) at temperatures of up to 1600°C. The heating/cooling rate was 7.5 to 10°C/min. As a reference substance, we used alumina powder. The sample weight was 50 to 150 mg. In addition, thermal analysis below 1400°C was performed with a Netzsch STA 449 system (Germany), which simultaneously recorded differential scanning calorimetry (DSC) curves and their derivatives. Powder samples weighing 30.00 ± 0.05 mg were loaded into a fused corundum crucible, heated in air from 20 to 1400°C at a rate of 10°C/min, and then cooled to 100°C at the same rate. As a reference, we used an empty corundum crucible of the same weight. The use of air instead of a reference substance was justified because the sample weight was smaller than the crucible weight by more than a factor of 6. In addition, this precluded the effects of the state of reference powder (particle size and tap density) and possible changes in its properties in the course of thermal analysis. The DSC curves obtained with no sample also indicated that the use of air as a reference had a positive effect at small sample weights. This approach was substantiated by Speyer [24].

The composition of $DyRhO_3$ was checked by gravimetry. We determined the weight of a $DyRhO_3$ sample and then the weight of the thermolysis products, Dy_2O_3 and Rh. To this end, the mixture of Dy_2O_3 and Rh was treated with concentrated nitric acid. The Dy_2O_3 fully dissolved, while rhodium metal remained intact, which allowed us to determine its weight and then calculate the weight of Dy_2O_3.

Full details of our experiments were described elsewhere [3, 5].

RESULTS AND DISCUSSION

The figure shows a schematic diagram of subsolidus phase relations in the Dy_2O_3–Rh_2O_3 system as a combination of two pseudobinary systems, Dy_2O_3–Rh and Dy_2O_3–Rh_2O_3, in the Dy–Rh–O ternary. A key feature of this representation is that the reversible dissociation of solid oxides is thought of as a phase transition, but the gas phase (oxygen) is left out of consideration. Phase equilibria in a ternary system can then be represented by a combination of two binaries, which makes it possible to obtain a clear schematic phase diagram in two dimensions. This approach to representing phase relations was first used by Muan and Gee [25] in studies of systems containing iron oxides. Schneider *et al.* [26] were the first to apply this method to systems containing platinum-metal oxides.

According to the phase diagram in the figure, the stable phases in the subsolidus region of the Dy_2O_3–Rh_2O_3 system are Dy_2O_3 (*C* form), β-Rh_2O_3, Rh, and $DyRhO_3$. There is also a metastable phase, α-Rh_2O_3. The ternary system Dy–Rh–O is monovariant when three solid phases are in equilibrium with the gas phase (oxygen). In that case, at a fixed oxygen partial pressure, three condensed phases coexist only at a certain temperature. In connection with this, three-phase equilibria in the phase diagram are represented by horizontal solid lines. The dashed line in the figure represents the monotropic polymorphic transition

$$\alpha\text{-}Rh_2O_3 \longrightarrow \beta\text{-}Rh_2O_3. \quad (1)$$

The metastable polymorph α-Rh_2O_3, which has the corundum (hexagonal) structure [22], transforms irreversibly into the stable polymorph β-Rh_2O_3, whose orthorhombic structure is also derived from the corundum structure [23]. The main features of this monotropic phase transition were studied earlier [21, 27–31]. The temperature range and rate of transformation (1) depend on the chemical composition, structure, and particle size of the starting α-Rh_2O_3, which, in turn, are determined by the synthesis procedure and conditions. For the rhodium oxide synthesized in this work, transformation (1) is detected easily after firing α-Rh_2O_3 above 750°C. Above 1030°C, we observe irreversible thermal dissociation according to the scheme

$$\beta\text{-}Rh_2O_3 = 2Rh + \frac{3}{2}O_2. \quad (2)$$

Equilibrium (2) and some of its thermodynamic features have been studied in detail [27–33]. Using earlier data [28, 32], one can evaluate the dissociation temperature of β-Rh_2O_3 in air at normal pressure, i.e., at an oxygen partial pressure of 0.21×10^5 Pa. The values thus obtained, 1034 and 1033°C, agree well with the 1042°C reported by Jacob and Sriram [33]. According to the DTA, DSC, and high-temperature x-ray diffraction (XRD) results obtained in [29–31], the temperature of equilibrium (2) in air is 1030 ± 5°C.

At temperatures of up to 1600°C, $DyRhO_3$ also undergoes only one chemical transformation: reversible thermal dissociation according to the scheme

$$DyRhO_3 = \frac{1}{2}Dy_2O_3 + Rh + \frac{3}{4}O_2. \quad (3)$$

The thermal dissociation of dysprosium rhodite shows up as a large endotherm in the DTA curve and a sharp weight loss of 7.58% in the TG curve. This values agrees well with the 7.66% following from scheme (3). The weight loss is well seen in the TG curve starting at 1345°C and in the DTG curve starting at 1320°C. In the DSC and derivative curves, the endothermic event begins at 1345°C. After annealing single-phase

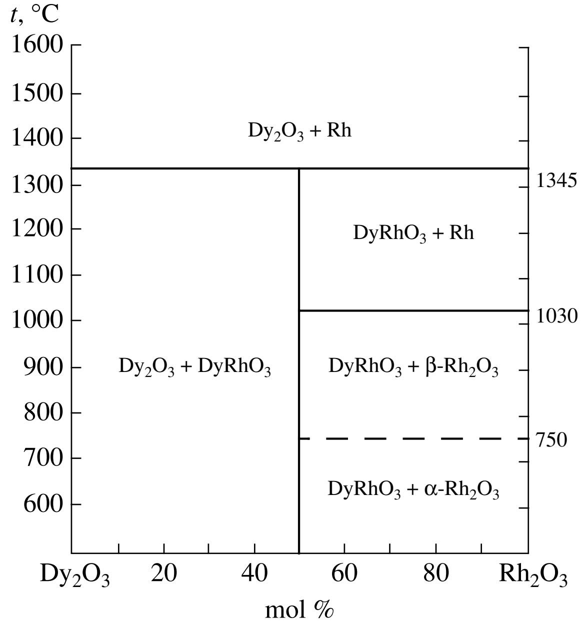

Schematic diagram of subsolidus phase relations in the Dy_2O_3–Rh_2O_3 system; the dashed line represents the irreversible polymorphic phase transition of Rh_2O_3.

$DyRhO_3$ samples above 1350°C, XRD patterns show sharp peaks due to large, well-crystallized rhodium particles and the so-called *C*-form of Dy_2O_3, which has a cubic structure [34]. In the range 1345–1600°C, these substances are nonreactive with one another and atmospheric oxygen. At the same time, after long-term (more than 100 h) firing of a mixture of Dy_2O_3 and fine-particle rhodium at 1320°C in air, XRD indicated the formation of $DyRhO_3$. Thus, our XRD and thermal analysis results for annealed and quenched samples confirm scheme (3) and indicate that the temperature of this equilibrium is 1345 ± 10°C.

Note that the thermal decomposition of $DyRhO_3$ by reaction (3) is similar to that of β-Rh_2O_3 by reaction (2). The two oxides dissociate reversibly with the formation of rhodium metal and oxygen, but the decomposition temperature of $DyRhO_3$ is substantially higher than that of Rh_2O_3.

Also of importance are the following findings: After heating rhodium(III) oxide to above 1030°C, XRD indicated the presence of well-crystallized, large-particle rhodium: the diffraction peaks from rhodium were much sharper than those from fine-particle rhodium. Fine-particle rhodium can easily be oxidized to single-phase β-Rh_2O_3, while well-crystallized, large-particle rhodium cannot be oxidized to Rh_2O_3, even at very long (500 h) annealing times in air or flowing oxygen at temperatures of up to 1000°C. The same was observed for equilibrium (3). These results indicate that the equilibration time for equilibria (2) and (3) depends significantly on the particle size of metallic rhodium.

Thus, the Dy_2O_3–Rh_2O_3 system contains only one mixed oxide: $DyRhO_3$. The chemical analysis data for $DyRhO_3$ agree well (to within 0.2%) with the nominal composition. Our powder XRD results confirm earlier reports [15–21] that $DyRhO_3$ crystallizes in the $GdFeO_3$ structure (orthorhombically distorted perovskite). Single-phase $DyRhO_3$ samples consist of homogeneous, dark brown powder which is insoluble in water, mineral acids (HCl, HNO_3, H_2SO_4, H_3PO_4), and caustic alkalies (NaOH, KOH), as are other $LnRHO_3$ compounds [3–6]. Note that Rh_2O_3 also has extremely high acid and alkali stability.

The proposed subsolidus phase diagram of the Dy_2O_3–Rh_2O_3 system is similar in topology to the Ln_2O_3–Rh_2O_3 (Ln = La, Ho, Er, Yb, Lu) phase diagrams [1–6]. These phase diagrams differ only in the dissociation temperature of $LnRhO_3$, which decreases from 1450 to 1275°C in going from $LaRhO_3$ to $LuRhO_3$ [1–6]. The phase diagram in the figure represents phase relations in air at normal pressure, i.e., at an oxygen partial pressure of 0.21×10^5 Pa. Clearly, the dissociation temperatures of β-Rh_2O_3 and $DyRhO_3$ depend on the oxygen partial pressure. According to Bayer and Wiedemann [28], increasing the oxygen partial pressure from 10^3 to 0.96×10^5 Pa increases the equilibrium dissociation temperature of rhodium(III) oxide from 900 to 1126°C. For $DyRhO_3$, such experimental data are not available in the literature. As reported by Jacob and Waseda [2], the dissociation temperature of the analogous perovskite oxide $LaRhO_3$ rises from 1455 to 1570°C as the oxygen partial pressure is raised from 0.21×10^5 to 10^5 Pa. Thus, as pointed out in many studies [1–6, 27–33, 35–37], the dissociation temperature of rhodium oxides in such systems depends significantly on oxygen partial pressure, as do their temperature and composition stability limits.

CONCLUSIONS

The present results confirm the close physicochemical similarity between the platinum metal–oxygen and base metal–platinum metal–oxygen systems and some inherent features of oxides in such systems [1–6, 18, 21, 26, 29–31, 35–38].

Subsolidus phase relations in binary oxide systems containing platinum-metal oxides are dominated by the physicochemical nature of the noble-metal oxide and depend much weaker on the base-metal oxide.

Most simple and double oxides of platinum metals exhibit polymorphism and/or undergo reversible thermal dissociation. Melting is atypical of both simple and double oxides of platinum metals.

Simple oxides of platinum metals decompose reversibly into the metal and oxygen (of the 15 solid simple oxides of platinum metals, the only exceptions are RuO_4, OsO_4, and OsO_2). Double oxides of platinum metals typically dissociate into the metal, oxygen, and a base-metal oxide. In most cases, the double oxides dissociate at higher temperatures than do the corresponding simple oxides. The highest thermal stability is offered by ruthenium, rhodium, and iridium oxides.

The great majority of the double oxides existing in base metal–platinum metal–oxygen systems inherit their physicochemical properties from the corresponding simple oxides of platinum metals. In particular, there is a strong correlation between the chemical and thermal stabilities of simple and mixed oxides of platinum metals.

ACKNOWLEDGMENTS

We are grateful to V.F. Popova, A.E. Lapshin, and D.P. Romanov for their assistance in the experimental work. We are also indebted to M.I. Morozov for providing us with preprints of reports needed for our work.

REFERENCES

1. Shevyakov, A.M., Skrobot, V.N., and Fedorov, N.F., Phase Equilibria in the System La_2O_3–Rh_2O_3, *Dokl. Akad. Nauk SSSR*, 1978, vol. 241, no. 2, pp. 423–425.
2. Jacob, K.T. and Waseda, Y., Phase Relations in the System La–Rh–O and Thermodynamic Properties of $LaRhO_3$, *J. Am. Ceram. Soc.*, 1995, vol. 78, no. 2, pp. 440–444.
3. Skrobot, V.N. and Grebenshchikov, R.G., Phase Relations in the System Yb_2O_3–Rh_2O_3, *Zh. Prikl. Khim.* (S.-Peterburg), 1999, vol. 72, no. 8, pp. 1247–1250.
4. Skrobot, V.N. and Grebenshchikov, R.G., Phase Relations in the System Lu_2O_3–Rh_2O_3, *Zh. Prikl. Khim.* (S.-Peterburg), 2000, vol. 73, no. 11, pp. 1767–1769.
5. Skrobot, V.N., Subsolidus Phase Relations in the Ho_2O_3–Rh_2O_3, *Zh. Neorg. Khim.*, 2002, vol. 47, no. 12, pp. 2041–2045.
6. Skrobot, V.N., Kuchaeva, S.K., Romanov, D.P., and Grebenshchikov, R.G., Subsolidus Phase Relations in the System Er_2O_3–Rh_2O_3, *Zh. Prikl. Khim.* (S.-Peterburg), 2003, vol. 76, no. 7, pp. 1063–1066.
7. Watson, P.R. and Somorjai, G.A., The Formation of Oxygen-Containing Organic Molecules by the Hydrogenation of Carbon Monoxide Using a Lanthanum Rhodate Catalyst, *J. Catal.*, 1982, vol. 74, no. 2, pp. 282–295.
8. Jarret, H.S., Sleight, A.W., Kung, H.H., and Gillson, J.L., Photoelectrochemical and Solid-State Properties of $LuRhO_3$, *J. Appl. Phys.*, 1980, vol. 51, no. 7, pp. 3916–3925.
9. Schinzer, C., Spin-Glass Behaviour of Disordered Perovskite $LaNi_{1/2}Rh_{1/2}O_3$, *J. Alloys Compd.*, 1999, vol. 288, no. 1/2, pp. 65–75.
10. Schinzer, C., A New Ferromagnetic Perovskite: $LaMn_{1/2}Rh_{1/2}O_3$, *J. Phys. Chem. Solids*, 2000, vol. 61, no. 10, pp. 1543–1551.
11. Guilhaume, N. and Primet, M., Three-Way Catalytic Activity and Oxygen Storage Capacity of Perovskite $LaMn_{0.976}Rh_{0.024}O_{3+\delta}$, *J. Catal.*, 1997, vol. 165, no. 2, pp. 197–204.
12. Mary, T.A. and Varadaraju, U.V., Orthorhombic–Tetragonal and Semiconductor–Metal Transition in the $La_{1-x}Sr_xRhO_3$, *J. Solid State Chem.*, 1994, vol. 110, no. 1, pp. 176–179.
13. Shimura, T., Itoh, M., Inaguma, Y., and Nakamura, T., Preparation and Electronic Properties of $Sr_{2-x}La_xRhO_4$, *Phys. Rev. B: Condens. Matter,* 1994, vol. 49, no. 8, pp. 5591–5598.
14. Layland, R.C., Kirkland, S.L., and zur Loye, H.C., Synthesis, Characterization, and Magnetic Properties of New Rh(III) Compounds with the K_4CdCl_6 Structure-Type Sr_3MRhO_6 (M = Sm, Eu, Tb, Dy, Ho, Er, and Yb), *J. Solid State Chem.*, 1998, vol. 139, no. 1, pp. 79–84.
15. Shannon, R.D., Cell Dimensions of Rare Earth Orthorhodites, *Acta Crystallogr., Sect. B: Struct. Crystallogr. Cryst. Chem.*, 1970, vol. 26, no. 4, pp. 447–449.
16. Shaplygin, I.S. and Lazarev, V.B., Electrical Properties of Mixed Oxides of Platinum Metals, *Dokl. Akad. Nauk SSSR*, 1974, vol. 218, no. 3, pp. 624–626.
17. Shaplygin, I.S. and Lazarev, V.B., Physicochemical Properties of Orthorhombic $MRhO_3$ Perovskites, *Vsesoyuznoe soveshchanie po khimii tverdogo tela* (All-Union Conf. on Solid-State Chemistry), Sverdlovsk–Pervoural'sk, 1975, part 2, p. 68.
18. Lazarev, V.B. and Shaplygin, I.S., Electrical Properties of Mixed Oxides, *Zh. Neorg. Khim.,* 1978, vol. 23, no. 2, pp. 291–303.
19. Lazarev, V.B. and Shaplygin, I.S., Electrical Conductivity of Platinum Metal–Base Metal Double Oxides, *Izv. Akad. Nauk SSSR, Neorg. Mater.*, 1978, vol. 14, no. 11, pp. 1942–1949.
20. Lazarev, V.B. and Shaplygin, I.S., Electrical Conductivity of Platinum Metal–Nonplatinum Metal Double Oxides, *Mater. Res. Bull.*, 1978, vol. 13, no. 3, pp. 229–235.
21. Shaplygin, I.S., Prosychev, I.I., and Lazarev, V.B., Chemistry and Properties of Mixed Rhodium Oxides, *Zh. Neorg. Khim.*, 1986, vol. 31, no. 11, pp. 2870–2875.
22. Coey, J.M.D., The Crystal Structure of Rh_2O_3, *Acta Crystallogr., Sect. B: Struct. Crystallogr. Cryst. Chem.*, 1970, vol. 26, no. 11, pp. 1876–1877.
23. Biesterbos, J.W.M. and Hornstra, J., The Crystal Structure of the High-Temperature, Low-Pressure Form of Rh_2O_3, *J. Less-Common Met.*, 1973, vol. 30, no. 1, pp. 121–125.
24. Speyer, R.F., *Thermal Analysis of Materials*, New York: Marcel Dekker, 1994.
25. Muan, A. and Gee, C.L., Phase Equilibrium Studies in the System Iron Oxide–Al_2O_3 in Air and at 1 atm. O_2 Pressure, *J. Am. Ceram. Soc.*, 1956, vol. 39, no. 6, pp. 207–214.
26. Schneider, S.J., Waring, J.L., and Tressler, R.E., Phase Relations between Iridium and the Sesquioxides in Air, *J. Res. Natl. Bur. Stand., Sect. A,* 1965, vol. 69, no. 3, pp. 245–254.

27. Muller, O. and Roy, R., Formation and Stability of the Platinum and Rhodium Oxides at High Oxygen Pressures and Structures of Pt_3O_4, β-PtO_2, and RhO_2, *J. Less-Common Met.*, 1968, vol. 16, no. 2, pp. 129–146.
28. Bayer, G. and Wiedemann, H.G., Bilding und thermische Stabilitat von Rhodium-Oxiden, *Thermochim. Acta,* 1976, vol. 15, no. 2, pp. 213–226.
29. Skrobot, V.N. and Grebenshchikov, R.G., Phase Relations in the System CaO–Rh_2O_3, *Zh. Neorg. Khim.*, 1989, vol. 34, no. 8, pp. 2127–2130.
30. Skrobot, V.N., Romanov, D.P., Kuchaeva, S.K., and Grebenshchikov, R.G., X-ray Powder Diffraction Study of the System Rh–O, *Int. Conf. on Powder Diffraction and Crystal Chemistry*, St. Petersburg, 1994, p. 81.
31. Skrobot, V.N. and Grebenshchikov, R.G., Phase Relations in the System MgO–Rh_2O_3–Rh, *Zh. Neorg. Khim.*, 1997, vol. 42, no. 11, pp. 1908–1911.
32. Schmahl, N.G. and Minzl, E., Die thermische Zersetzung des Rhodium (III)-Oxids und deren Beeinflussung durch Legierungsbildung mit Platin und Palladium, *Z. Phys. Chem.*, 1964, vol. 41, no. 1/2, pp. 78–96.
33. Jacob, K.T. and Sriram, M.V., Phase Relations and Gibbs Energies in the System Mn–Rh–O, *Metall. Mater. Trans. A*, 1994, vol. 25, no. 7, pp. 1347–1357.
34. Glushkova, V.B., *Polimorfizm okislov redkozemel'nykh elementov* (Polymorphism of Rare-Earth Oxides), Leningrad: Nauka, 1967.
35. Skrobot, V.N. and Grebenshchikov, R.G., Phase Relations in Oxide Systems Containing Platinum Metals, *Mezhdunarodnaya konferentsiya po khimii tverdogo tela* (Int. Conf. on Solid-State Chemistry), Odessa, 1990, part 2, p. 86.
36. Skrobot, V.N. and Grebenshchikov, R.G., Phase Relations in Oxide Systems Containing Platinum-Metal Oxides, *Mezhdunarodnaya konferentsiya po vysokotemperaturnoi khimii silikatov i oksidov* (Int. Conf. on High-Temperature Chemistry of Silicates and Oxides), St. Petersburg, 1998, p. 101.
37. Skrobot, V.N., Kuchaeva, S.K., Romanov, D.P., and Grebenshchikov, R.G., Thermal Stability of Platinum-Metal Oxides, *Mezhdunarodnaya konferentsiya po vysokotemperaturnoi khimii silikatov i oksidov* (Int. Conf. on High-Temperature Chemistry of Silicates and Oxides), St. Petersburg, 2002, p. 115.
38. Shevyakov, A.M., Skrobot, V.N., and Fedorov, N.F., Synthesis of Mixed Oxides in Systems Based on Platinum-Metal and Rare-Earth Oxides, *Dokl. Akad. Nauk SSSR,* 1977, vol. 235, no. 2, pp. 372–375.